Properties of an electron in a quantum double well driven by a strong laser: Localization, low-frequency, and even-harmonic generation

Raanan Bavli and Horia Metiu
Department of Chemistry and Physics, University of California, Santa Barbara, California 93106*
(Received 26 August 1992; revised manuscript received 10 November 1992)

We study how a strong semi-infinite laser pulse affects an electron confined by a potential whose parameters mimic an AlAs-GaAs-AlAs double quantum well. Interesting phenomena take place for special values of laser frequency, intensity, and pulse rise time. There are values of these parameters for which the dipole moment of the system has a low-frequency Fourier component whose magnitude is higher than that of the fundamental (i.e., the component having the same frequency as the laser). For other parameter values, the low-frequency component disappears and the Fourier transform of the dipole moment has a large zero-frequency component and intense even-harmonic components (i.e., with frequency $2n\omega$, where n is an integer and ω is the laser frequency). The presence of the even harmonics is intriguing: The system has inversion symmetry and even harmonics are forbidden by symmetry rules valid to all orders in perturbation theory. Finally, a laser pulse with well-chosen parameters can drive an electron that was initially in a delocalized eigenstate, to a state in which it is almost completely localized in one well. These processes are systematically investigated by numerical calculations and are rationalized with the help of a simple model which predicts the qualitative behavior observed numerically. The model suggests that these phenomena occur at those values of the parameters for which two Floquet states having different generalized parities become degenerate or nearly degenerate. This condition is rather general and we see no reason why it will not be fulfilled in systems other than double quantum wells (e.g., atoms or molecules).

PACS number(s): 42.65.Ky, 42.50.Hz, 03.65.Ge, 33.80.Wz

I. INTRODUCTION

We study the effect of a strong laser on an electron confined by a potential whose parameters are chosen to mimic an AlAs-GaAs-AlAs double quantum well [1]. Recent work suggested that such a system may have interesting properties. Grossmann and co-workers [2(a)–(c)] have examined the behavior of an electron that is initially localized in one of the wells of a quartic double well and is then driven by a strong cw laser. In the absence of radiation, the electron oscillates back and forth between the wells. A laser with appropriate power and frequency can prevent this motion [2(a)–(c)] and force the electron to stay in the initial well. These papers present numerical results as well as a nonperturbative analysis. The same phenomena were examined for a two-level approximation [2d]. If the electron-laser interaction energy is much higher than the energy difference between the lowest two energy eigenstates of the bare [3] system, the laser parameters for which this localization occurs can be obtained from a simple formula [2,4].

The calculations presented here extend the previous work and document the existence of several other interesting phenomena.

(1) Instead of assuming that the system is initially localized in a well (a condition that is rather difficult to achieve in the laboratory), we consider an electron that starts in a delocalized energy eigenstate of the bare Hamiltonian, and show that a pulse with carefully chosen parameters can localize the electron in one well and keep it there. One of the intriguing results of the numerical calculations is that localization is created or is maintained by the laser only if its frequency ω and intensity I take specific values. For a square laser pulse, these values are located along a family of lines in the plane $\{\omega,I\}$. A simple formula [2d,4a,4b] for these lines, based on perturbation-theory analysis of a two-level system, predicts fairly well most of the values of $\{\omega,I\}$ for which we observed localization in the numerical work presented here. If the system is driven by a Gaussian semiinfinite pulse, the rise time τ of the pulse is also an important parameter. To achieve localization $\{\omega,I\}$ must be on the lines mentioned above and, in addition, τ must have certain values.

(2) For parameters values along the lines in the $\{\omega,I\}$ space that were mentioned above, the Fourier transform of the dipole induced by the laser has finite components at the frequencies $2n\omega$ (n is an integer). We call this phenomenon even-harmonic generation (EHG). The double well in which the electron moves is symmetric, and therefore the bare Hamiltonian is invariant with respect to a sign change in the electron position. Perturbation theory to all orders shows that such a system cannot produce even harmonics. Because of this, the existence of EHG is surprising. The violation of the selection rule takes place at the same points in the parameter space where electron localization occurs.

(3) The dipole of the structure has low-frequency components. This frequency depends on $\{\omega,I\}$, and can be tuned, by changing these parameters, to be as close to zero as one wishes. We call this process low-frequency

generation (LFG).

The EHG, the static dipole and the localization appear, and LFG disappears, at the same points in the $\{\omega,I\}$ plane. Intense LFG is seen near these points. These phenomena are documented by solving the time-dependent Schrödinger equation numerically. By treating these calculations as experiments, we infer rules of behavior for the Fourier components of the induced dipole (Sec. VI). The same rules are then derived from an analysis in terms of the Floquet states of the system. This extends the analysis presented in previous work [2,4], which showed that localization is related to the accidental degeneracy of the Floquet quasienergies.

II. MODEL

The Hamiltonian of the system studied here is

$$H(t)=H_0+V(t)=-\left[\frac{\hbar^2}{2m^*}\right]\frac{d^2}{dx^2}+V_0+V(t)\ . \tag{1}$$

This describes an electron having an effective mass $m^*=0.067$ m (m is the electron mass) trapped in the potential V_0, shown in Fig. 1. The parameters of the potential are typical of an $Al_yGa_{1-y}As$ double quantum well [1]. The gap between the ground and the first excited state of the bare Hamiltonian H_0 is 16.68 meV (134.5 cm^{-1}); that between the first and the second excited state is 193.3 eV (1558.9 cm^{-1}). The laser electron interaction is

$$V(t)=exE(t)\ . \tag{2}$$

The electric field of the laser is either

$$V(t)=\begin{cases}0, & t\le 0\\ exE_0\cos[\omega t+\delta], & t\ge 0\end{cases} \tag{3}$$

or

$$V(t)=\begin{cases}exE_0\exp[-(t-t_0)^2/(2\tau^2)]\cos[\omega t+\delta], & t\le t_0\\ exE_0\cos[\omega t+\delta], & t\ge t_0\ .\end{cases} \tag{4}$$

Equation (3) represents a square pulse, and Eq. (4) a semi-infinite Gaussian pulse. The parameter E_0 is specified by giving the laser intensity $I=2\epsilon cE_0^2$. If E_0 is given in statvolt/cm, $c=3\times10^{10}$ cm/sec, and $\epsilon=1/(4\pi)$, then I is obtained in erg sec^{-1} cm^{-2}.

This model provides only a schematic description of an electron in a double quantum well. We neglect the motion of the electron parallel to the well and assume that the effective mass is the same in the wells and under the barrier. By using infinitely high walls, we prevent the escape of the electron from the two-well system. In reality, a laser acting for a sufficiently long time on an electron in a real well will cause it to "photodissociate." We also neglect energy loss and dephasing processes which, if included, would destroy phase coherence, diminish the electron localization, and broaden the spectroscopic features obtained with our simple model.

In a more realistic calculation, the well modifies the electromagnetic field so the force acting on the electron is not that of the incoming laser. In principle, we should solve Maxwell equations with the boundary conditions appropriate for the double-well system and with a nonlinear susceptibility calculated by solving simultaneously and self-consistently the time-dependent Schrödinger equation for the electron. Such calculations are difficult, and they are avoided as long as there is no compelling reason for performing them. One hopes that, as long as the laser does not excite the electromagnetic resonances of the structure, the simple model describes semiquantitatively the behavior of the electron.

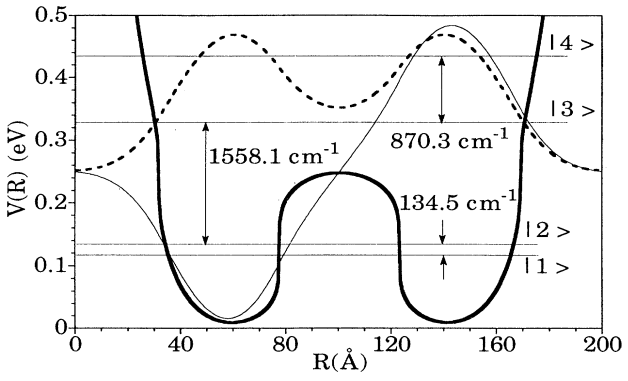

FIG. 1. Potential energy and the lowest-energy eigenstates. The energies of the first four states are shown by the horizontal lines. The barrier height is 240 meV and its width is 45 Å. The wells have about the same width as the barrier. The potential energy is $V(R)=1000\{[(D+|D|)/2]^{1/4}-[(|D|-D)/2]^{1/4}+1\}+\exp[30(R/L-\frac{1}{2})]$, where L is the total length of the structure ($=96\pi$ Å), and $D\equiv\cos(6.6R/L-1.3\pi)$. The broken and solid lines show the lower two states of the system.

III. METHOD OF COMPUTATION

The results reported here are obtained by solving numerically the time-dependent Schrödinger equation. The evolution of the wave function is calculated by using repeatedly the short-time propagator

$$|\psi(t+\delta t)\rangle=\exp[-iH(t)\delta t]|\psi(t)\rangle\ , \tag{5}$$

where the time-dependent Hamiltonian H is given by Eqs. (1)–(4). The exponential operators are evaluated by a fast-Fourier-transform method proposed by Fleck, Morris, and Feit [5a], and implemented as described by Heather and Metiu [6]. The time-dependent wave function is used to calculate the probability that the electron is located in the left well:

$$P_L(t)=\int_{-\infty}^{L/2}dx\ \psi^*(x,t)\psi(x,t)\ , \tag{6}$$

and the dipole induced by the action of the laser on the electron:

$$\mu(t)=e\int_{-\infty}^{\infty}dx\ \psi^*(x,t)x\psi(x,t)\ . \tag{7}$$

IV. USE OF RADIATION TO MAINTAIN THE INITIAL LOCALIZATION

We study in this section a system whose state at $t=0$ is $|L\rangle=(|1\rangle-|2\rangle)/2^{1/2}$, where $|1\rangle$ and $|2\rangle$ are the two lowest-energy eigenstates of the electron in the absence of the laser. In this state, the electron is localized in the left well with a probability $P_L(t=0)=0.987$. This is not a two-level calculation. All the results are obtained by solving numerically the time-dependent Schrödinger equation for the double well. By numerical experimentation, we find the laser intensity, frequency, and phase for which a cw laser will keep the electron in the left well. This was also done in the previous work [2], but there are some differences. In our calculation, a square laser pulse is turned on at $t=0$. In the previous calculations [2], the laser was turned on in the infinite past, and the electron was in the left well at $t=0$. Furthermore, we study the role played by the laser phase, and monitor the time evolution of the system continuously rather than stroboscopically.

The frequencies at which the laser maintains localization range between $\varepsilon/5$ and 11ε, where $\varepsilon=16.68$ meV (134.5 cm^{-1}) is the energy difference between the ground and the first excited state of the bare electron. One would naively expect that the laser frequencies capable of maintaining localization should be related in a simple way to the frequency of the well-to-well oscillation of the electron in the absence of the laser, which in turn is determined by ϵ. No such relationship is observed. The laser is sufficiently strong to make ε, which characterizes the bare electron, a physically irrelevant parameter. Table I lists the frequencies for which a laser of intensity 34.722 MW/cm^2 maintains the initial electron localization, together with the time-averaged probability of being in the initial well. The latter is never less than 70% at any time, and its time average is above 80%. A similar behavior, at other frequencies, is observed if the laser intensity is smaller by a factor of 10 or 100.

A simple formula for the laser frequency and intensity for which the laser maintains the initial localization has been derived in Ref. [2d], by a perturbation-theory analysis of a two-level model. An important prediction of this analysis is that the parameter controlling the localization is the ratio $2E\mu_{12}/\hbar\omega$; localization takes place when this parameter is equal to one of the zeros of the Bessel function J_0. At the high laser intensity used here, one is not sure that the double-well–laser interaction can be described by using two levels only. In Table I we show the value of the parameter $2E\mu_{12}/\hbar\omega$ at the localization points in out numerical calculations and the closest value given by the formula derived in Ref. [2d]. Most of the numerical results agree remarkably well with the ones provided by the simple formulas. However, not all is well. The equation predicts that no localization will occur if the parameter $2E\mu_{12}/\hbar\omega$ is smaller than 2.4 (which is the first zero of J_0). The numerical calculations found (see Table I) four exceptions to this rule.

The time evolution of the probability $P_L(t)$ that the electron is in the left well is shown in Fig. 2 for a square pulse with a photon energy of 228.28 cm^{-1}, an intensity of 34.722 MW/cm^2 and the phase $\delta=1.5\pi$. We also show $P_L(t)$ for the same initial state, when the laser is not on. Figure 3 presents a second example. The conditions are the same as in Fig. 2, except for the laser frequency. Photons of energy 841.42 cm^{-1} localize the electron, but

TABLE I. Frequencies for which a laser of intensity 34.722 MW/cm^2 maintains the initial localization. The third column is the time-averaged probability of being in the initial well. Our parameters values given in the fourth column are compared with ones from Ref. [2(d)], as discussed in the text.

Set No.	$\hbar\omega$ (cm^{-1})	$\langle P_L\rangle$	$2E\mu/\hbar\omega$	Ref. [2(d)]
1	26.280	0.833	62.79	62.05
2	27.679	0.838	59.61	58.91
3	29.236	0.844	56.44	55.77
4	30.979	0.850	53.26	52.62
5	32.944	0.855	50.08	49.48
6	35.174	0.859	46.91	46.34
7	37.728	0.868	43.73	43.20
8	40.684	0.874	40.56	40.06
9	44.142	0.880	37.38	36.92
10	48.244	0.887	34.20	33.78
11	53.187	0.893	31.02	30.63
12	59.261	0.900	27.84	27.49
13	66.903	0.906	24.66	24.35
14	76.813	0.912	21.48	21.21
15	90.176	0.919	18.30	18.07
16	109.11	0.871	15.12	14.93
17	138.50	0.928	11.91	11.79
18	190.28	0.921	8.67	8.65
19	309.78	0.904	5.33	5.52
20	628.73	0.830	2.62	2.40
21	841.42	0.891	1.98	
22	1339.3	0.815	1.24	
23	1443.8	0.806	1.15	
24	1560.8	0.793	0.94	

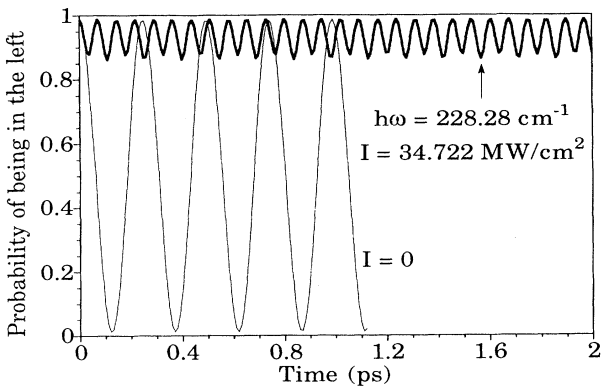

FIG. 2. Time evolution of the probability $P_L(t)$ that the electron is in the left well. At time zero, the electron was located in the left well, and it is driven with a square laser pulse that is turned on at $t=0$ has a frequency of 228.28 cm^{-1}, an intensity of 34.722 MW/cm^2, and the phase $\delta=1.5\pi$ [see Eq. (6)]. The thin line shows that, in the absence of the field, $P_L(t)$ oscillates with a period of about 250 fs.

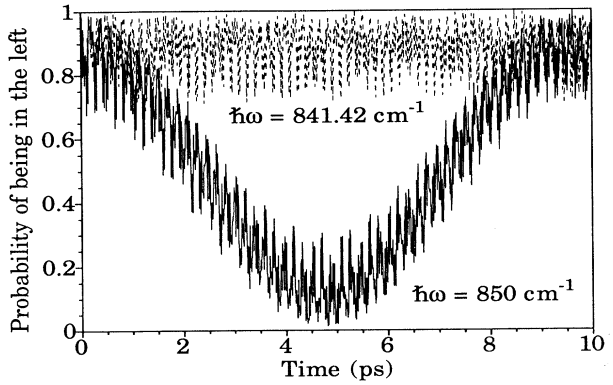

FIG. 3. Time evolution of the probability $P_L(t)$ that the electron is in the left well. At time zero, the electron was located in the left well, and it is driven with a square laser pulse that is turned on at $t=0$, has an intensity of 347.22 MW/cm^2, and the phase $\delta=1.5\pi$ [see Eq. (6)]. The upper curve corresponds to a frequency of 841.42 cm^{-1}, and the electron is localized. The lower curve corresponds to a frequency of 850.0 cm^{-1}, and the electron drifts from one well to another with a period of 9.5 ps, which corresponds to a frequency of 3.5 cm^{-1}.

those of 850.0 cm^{-1} do not. A detuning of only 8.58 cm^{-1} from the localization frequency causes the electron to oscillate between the wells with a period of 9.5 ps (3.5 cm^{-1} in frequency domain). This oscillation is much slower than that of a bare electron with the same initial state, which is about 250 fs. Thus, when the laser is unable to maintain localization, it is capable of inducing a low-frequency oscillation between the wells. This causes a large low-frequency component in the induced dipole.

Next we check how the ability of the laser to maintain the localization of the electron depends on the phase δ of the electric field. The time-dependent Schrödinger equation is invariant to a change in the origin of time scale,

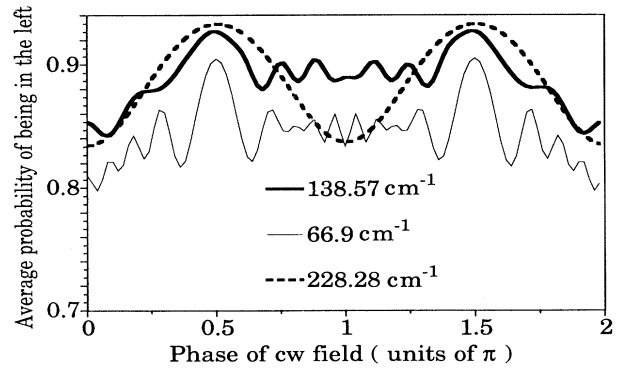

FIG. 4. Time-averaged probability of being in the initial well as a function of the phase δ [see Eq. (6)] of the laser field. The electron was at $t=0$ in the left well. The laser intensity is 347.22 MW/cm^2, and the pulse is square and was turned on at $t=0$. The three curves correspond to the laser frequencies shown in the figure.

and one might think that the phase of the laser should make no difference. This is not the case. At time zero, the electron is localized in the left well and, in the absence of the laser, it would oscillate towards the right well and back. The magnitude and the direction of the electric field at time zero, which are both phase dependent, are important: it makes a difference whether the laser pushes the electron along its spontaneous motion or opposes it. This dependence is shown in Fig. 4, where the time-averaged probability of being in the left well is plotted versus the laser phase. Some localization is maintained at all phases, but its quality varies; it is best at $\delta=0.5\pi$.

One would naively think that the best way of maintaining localization is to time the oscillations of the electric field of the laser to oppose the electron motion whenever it tries to move away from the initial well. The calculations do not support this classical picture.

V. USE OF A SEMI-INFINITE LASER PULSE TO PREPARE AND MAINTAIN ELECTRON LOCALIZATION

It is very difficult to achieve experimentally the situation studied in Sec. IV. Localized states of the electron are as hard to prepare as they are hard to maintain. In this section, we consider the case when the electron is initially in an eigenstate of the bare system and the laser is a semi-infinite Gaussian pulse. The question is whether we can find pulse parameters for which electron localization is created and maintained. In Fig. 4, we show the dependence of the time-averaged probability P_L that the electron is in the left well, as a function of the rise time t of the semi-infinite Gaussian pulse defined by Eq. (7). The electron is initially in the ground state and it is equally distributed in the two wells. The pulse phase is $\delta=\pi-\omega t_0$, where t_0 is the time when the amplitude of the pulse reaches its constant value. This choice assures that, at t_0, the phase is π. We see that there are many values of the rise time t for which the localization is near 90% or 10%. The latter means that the electron is localized in the right well. The dependence of P_L on τ does not have to be as regular, as seen in Fig. 4(a). A change in laser frequency and intensity leads to the results shown in Fig. 4(b). Localization of at least $\sim$90% in one well was obtained for τ's as long as ten optical cycles when frequency of 66.9 cm^{-1} was used. For a laser frequency of 138.57 cm^{-1}, localization of at least $\sim$80% was obtained for τ's as long as 18 optical cycles.

It seems that the ability of the semi-infinite Gaussian pulse to create and maintain localization is confined to low frequencies. For laser frequencies larger than 138.57 cm^{-1}, we were unable to find even one value of τ for which an electron initially in $|1\rangle$ or $|2\rangle$ ends up being localized.

Several examples of the detailed evolution of $P_L(t)$ are shown in Fig. 5. In all the graphs, the Gaussian amplitude reaches a maximum at $t_0=3.5\tau$ and then levels off to a constant value. The value of t_0 for the upper curve in Fig. 5(a) is 585 fs. In the early times, when the laser intensity rises, $P_L(t)$ undergoes wild oscillations and the

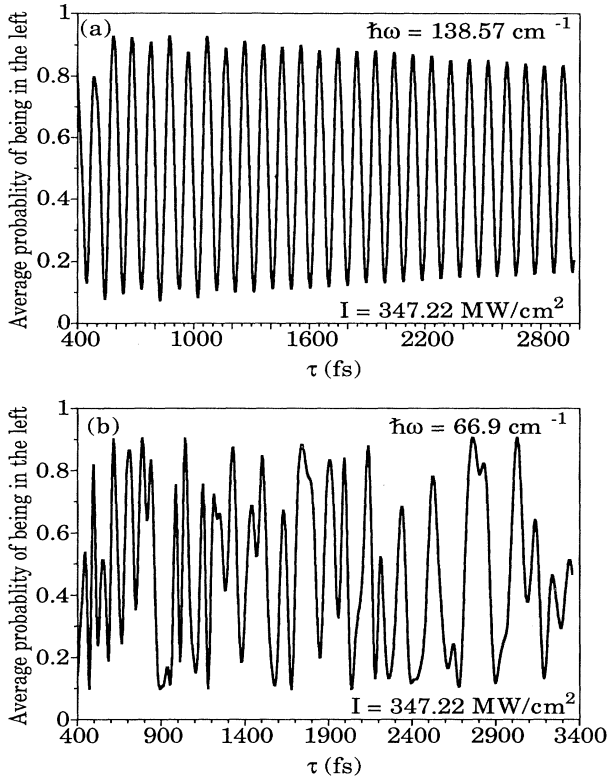

FIG. 5. Time-averaged probability P_L that the electron driven by a semi-infinite Gaussian pulse is in the left well, plotted as a function of the pulse rise time τ. The electron is initially in the bare ground state. The phase of the pulse is $\delta=\pi-\omega t_0$, where $t_0=3.5\ \tau$ is the time when the laser amplitude becomes constant. (a) The pulse frequency is 138.57 cm^{-1} and the intensity is $I=347.22$ MW/cm^2. (b) The pulse frequency is 66.9 cm^{-1} and the intensity is $I=347.22$ MW/cm^2.

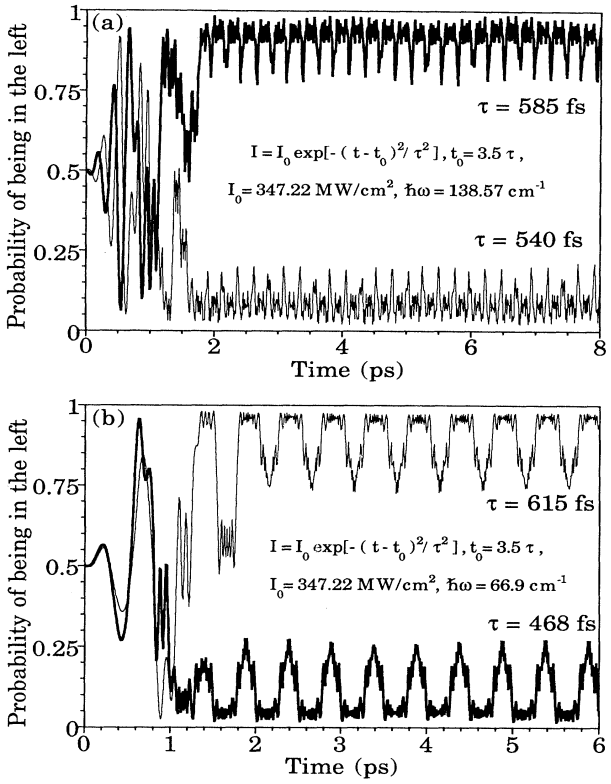

FIG. 6. Time dependence of the probability $P_L(t)$ for an electron driven by a Gaussian semi-infinite pulse. The relevant laser parameters are indicated in the figures. The phase is $\delta=\pi-\omega t_0$.

electron moves from one well to another. When the pulse settles to a constant value, $P_L(t)$ oscillates with a small amplitude around a mean value larger than 0.9. The second graph in Fig. 5(a) shows that if we change the rise time from $t=585$ fs to $\tau=540$ fs, but keep all other parameters unchanged, the electron will be localized in the right well. Figure 5(b) shows the results of similar calculations with a photon energy of 66.9 cm^{-1}.

The localization probability depends on the phase δ of the pulse (Fig. 6). A pulse that leads to electron localization in the left well for $\delta=-\omega t_0\pm\pi$ will localize the electron in the right well if the phase is changed to $\delta=\omega t_0\pm 2\pi$; if the phase differs from these two values, the localization is poor. The reason why a phase change can shift localization from one well to the other can be understood from the symmetry of the Hamiltonian.

Unless one works at a very low temperature, the excited state $|2\rangle$ is also populated in the bare system. For this reason, we have investigated the effect of a semi-infinite pulse on an electron that is initially in state $|2\rangle$. We find that a pulse having a set of parameters that localize an electron starting in $|1\rangle$ in the left well, will localize an electron starting in $|2\rangle$ in the right well. If the same pulse acts on an electron in thermal equilibrium, the population in the left well will exceed that in the right well by a Boltzmann (or a Fermi) factor.

VI. SPECTROSCOPIC PROPERTIES

In this section, we investigate the spectroscopic properties of an electron in a double well by calculating the evolution of the dipole moment $\mu(t)$. We are especially interested in what happens when the system is driven at values of $\{I,\omega\}$ that are nearly equal or equal to those at which the laser is capable of maintaining localization.

To identify the frequencies controlling the time evolution of $\mu(t)$, we calculate the Fourier transform [6]

$$\mu(\Omega)=\left|\int_{-\infty}^{+\infty}dt\, e^{-i\Omega t}W(t-t')\mu(t)\right| . \tag{8}$$

$\mu(t)$ is obtained from Eq. (7), and the time-dependent wave function is calculated numerically. The time t' and the width in the Gaussian window function $W(t-t')$ are chosen to include in the transform only those times when the pulse intensity is constant. $\mu(\Omega)$ has peaks of Gaussian shape (i.e., the transform of the window function) centered at the frequencies of the Fourier components of $\mu(t)$. In all the figures that follow, we give only the peak heights and positions.

To present the numerical results efficiently, we classify the Fourier components of $\mu(t)$ according to their frequency Ω. Four kinds of terms are possible; a static term ($\Omega=0$); pure-harmonic terms ($\Omega=n\omega$, $n=\pm1,\pm2,\ldots$); shifted-harmonic terms ($\Omega=n\omega\pm\Delta_{\alpha,\beta}$, $n=\pm1,\pm2,\ldots$ and $\alpha,\beta=1,2,\ldots$); and bandheads ($\Omega=\pm\Delta_{\alpha,\beta}$, $\alpha,\beta=1,2,\ldots$). The bandheads are shifted harmonics with $n=0$, but we prefer to list them as a separate category.

The quantities $\Delta_{\alpha,\beta}$ depend on the laser intensity and frequency. This can have important consequences. For example, for certain values of $\{\omega,I\}$, we can have $\Delta_{\alpha,\beta}(\omega,I)=0$, for a pair of indices α,β. We call the values of $\{\omega,I\}$ for which this equation is satisfied points of accidental degeneracy (AD). In general, the equation defines a family of curves in the $\{\omega,I\}$ plane.

In Fig. 7, we show $\mu(\Omega)$ for two laser powers and frequencies. We obtain a pure-harmonic progression, having the frequencies $\Omega=(2n+1)\omega$, and two shifted harmonics, having the frequencies $\Omega=2n\omega+\Delta$ and $2n\omega-\Delta$. In Fig. 7(a), $\Delta=36$ cm^{-1} and in Fig. 7(b), $\Delta=29.9$ cm^{-1}. Note the presence of low-frequency peaks at $\Delta=36$ cm^{-1} [in Fig. 7(a)] and $\Delta=29.9$ cm^{-1} [in Fig. 7(b)], which are bandheads and provide examples of the low-frequency-generation process mentioned in the Introduction. Perturbation theory suggests, and practice often confirms, that the intensity of the Rayleigh peak (at $\Omega/\omega=1$) tends to be the highest in a spectrum. This is not the case in Fig. 7. The low-frequency peaks have the highest intensity (note the logarithmic scale of the plot). Numerous calculations, whose results are not shown here, indicate that the LFG frequency depends on $\{I,\omega\}$ and can be tuned, by changing these parameters, to be as close to zero as one wants.

We have found that in all cases when intense LFG is present, the evolution of $P_L(t)$ is similar to that of the lower curve in Fig. 3: the electron density drifts slowly from one well to another. The dipole caused by this oscillations is very large, and this explains the high LFG intensity.

The transforms shown in Fig. 7 have a fairly large number of odd harmonics [i.e., pure harmonics with frequency $(2n+1)\omega$] and no even ones. Perturbation theory indicates that if the bare Hamiltonian does not change when x is replaced by $-x$, the dipole has no even-harmonic components. This widely used rule is valid to all orders in perturbation theory. In view of this, the results shown in Fig. 8 are surprising. In both cases

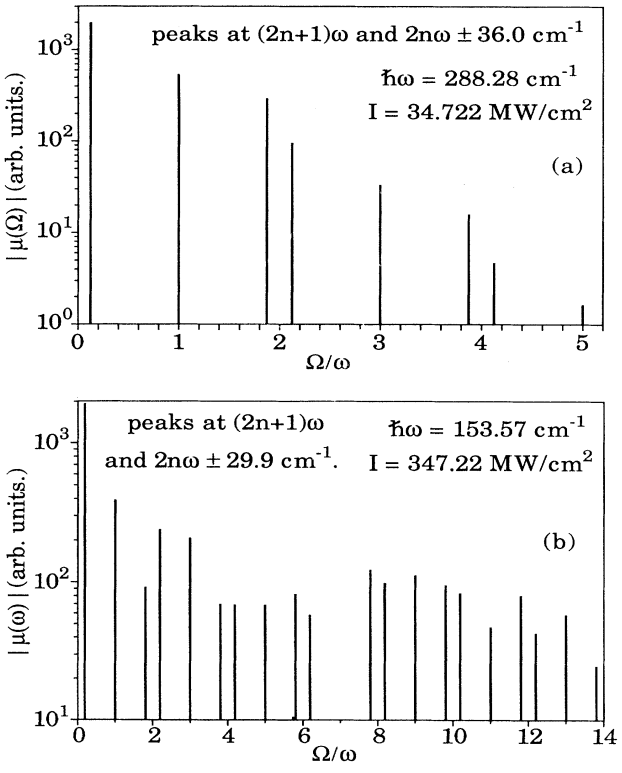

FIG. 7. Two examples of Fourier components of the dipole. The transform is defined by Eq. (12). The vertical lines are located at the maximum frequency, and their height is proportional to the peak intensity. The electron is initially in the bare ground state. The pulse is square and the phase is $\delta=1.5\pi$. (a) and (b) correspond to different laser frequencies and intensities (see the figure).

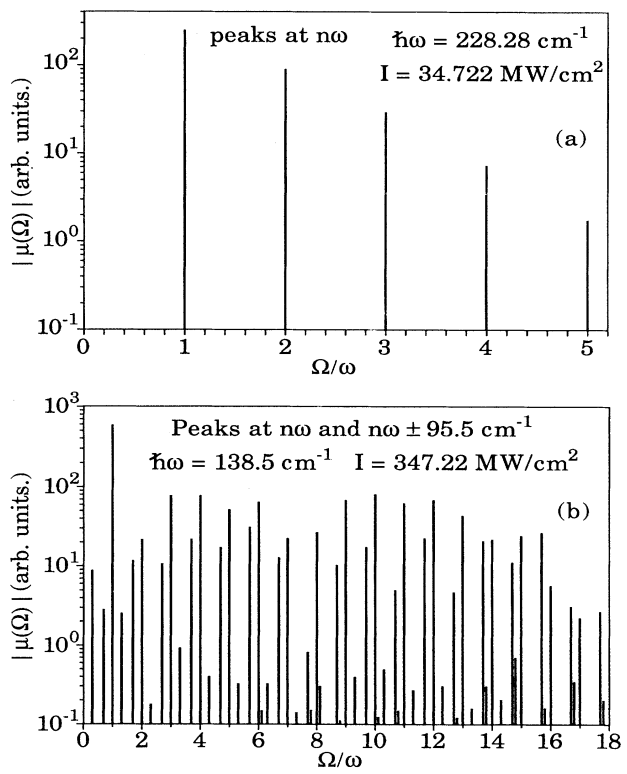

FIG. 8. Two examples of Fourier components of the dipole for cases of accidental degeneracy. (a) and (b) are for laser frequencies of 228.28 cm^{-1} and 138.5 cm^{-1} and the same intensities and phases as in Figs. 7(a) and 7(b), correspondingly. Note that in (b), the peaks at $(n\omega-95)$ cm^{-1} are much more intense than the peaks at $(n\omega-95)$ cm^{-1}.

we see that $\mu(\Omega)$ has intense peaks at the frequency $\Omega=2n\omega$. These are not confined to low values of n, nor does their intensity decrease with n, as perturbation theory would suggest; in one case, not shown here, the intensity of the twenty-second harmonic was close to that of the fundamental.

By numerical experimentation, we have found a number of propensity rules. These rules guided us to the classification and the nomenclature introduced at the beginning of this section. Much of the observed behavior of the spectrum is controlled by the behavior of the "shift frequencies" $\Delta_{\alpha,\beta}$. As $\{\omega,I\}$ approaches a point of accidental degeneracy (where $\Delta_{\alpha,\beta}\rightarrow 0$), the frequency of the LFG line goes to zero, the doublets corresponding to the shifted-harmonic terms $n\omega\pm\Delta_{\alpha,\beta}$ coalesce to give pure harmonics, and $\mu(t)$ acquires a static dipole moment [i.e., $\mu(t)$ equals a constant plus a time-dependent part]. The last effect is an indication of electron localization. We note that the ability of maintaining localization depends also on the phase of the laser, while the presence of EHG does not (however, the intensity of EHG does); the presence of EHG does not always imply that the laser will maintain a strong localization [i.e., with $P_L(t)$ larger than 0.9 at all times].

Finally, we have not observed shifted odd harmonics [i.e., $\Omega=(2n+1)\omega\pm\Delta$] at any parameter values, nor have we seen pure even harmonics for parameters that were not AD points.

The nomenclature used here is influenced by the laser parameters used in the calculations. The low-frequency component is low only because Δ is much smaller than ω; the phenomena described here may exist if $\omega\gg\Delta$, in which case the component of frequency $\Omega=\Delta$ might be viewed as a high-frequency component.

VII. INTERPRETATION

In this section, we show that the results presented in Sec. VI can be understood by using Floquet [7] theory. The Floquet analysis has been already used successfully to discuss laser localization in a two-level-system model [2d] and to analyze numerical results of interaction with double-well systems [2a–c]. Here we show that the LFG and EHG phenomena can be treated similarly. The Floquet theory shows [7] that one can write the solution of the time-depended Schrödinger equation as

$$\Psi(x,t)=\sum_{\alpha=1}^{\infty}A_\alpha\exp(-i\varepsilon_\alpha t)\Phi_\alpha(x,t)\ , \tag{9}$$

where the real numbers ε_α are the electron quasienergies, and the Floquet states $\Phi_\alpha(x,t)$ have the same period as the laser [i.e., $\Phi_\alpha(x,t)=\Phi_\alpha(x,t+2\pi/\omega)$]. If the laser has a constant amplitude, the coefficients A_α are independent of time. If the system is driven by a pulse, A_α become independent of time when the transients excited by turning on the pulse quiet down.

The periodic function Φ_α can be expanded in a Fourier series:

$$\Psi(x,t)=\sum_{\alpha=1}^{\infty}A_\alpha\exp(-i\varepsilon_\alpha t)\left[\sum_{n=-\infty}^{\infty}C(n,x;\alpha)\exp(in\omega t)\right]\ ; \tag{10}$$

the function $C(n,x;\alpha)$ is the nth Fourier coefficient in the expansion of $\Phi_\alpha(x,t)$. We call $C(n,x;\alpha)$ the Floquet modes of Φ_α.

Equation (10) allows us to write the time evolution of an operator $O(x)$, which depends on x only, as

$$\begin{aligned}O(t)&=\langle\Psi,t|O(x)|\Psi,t\rangle\\&=\sum_{\alpha=1}^{\infty}\sum_{\beta=1}^{\infty}A_\alpha^*A_B\exp[-i(\varepsilon_\beta-\varepsilon_\alpha)t]\\&\quad\times\sum_{n=-\infty}^{\infty}\sum_{m=-\infty}^{\infty}\exp[i(m-n)\omega t]\\&\qquad\times\int_{-\infty}^{\infty}dx\ C^*(n,x;\alpha)\\&\qquad\times O(x)C(m,x;\beta)\ .\end{aligned} \tag{11}$$

We are interested in two operators: $O(x)=\mu=ex$, which gives the dipole of the structure, and $O(x)=P_L(x)$, which gives the probability that the electron is in the left well [$P_L(x)$ is one when the electron is in the left well, and zero otherwise].

Equation (11)—which is a standard formula in Floquet theory—gives the time evolution of an observable as a sum of exponentials, even though the Hamiltonian is time dependent. The time scales on which various electron observable change are given in terms of differences between the quasienergies ε_α and of multiples of the laser frequency. The eigenstates of H_0 cannot provide a similar description since the laser is strong. Those of $H(t)$ are time dependent and have no clear connection with the time scales on which $\mu(t)$ evolves.

The qualitative features of the numerical results presented earlier in this article can be understood from Eq. (11) and the symmetry of the Hamiltonian. One can show that the transformation $\{x,t\}\rightarrow\{x,t+(2j+1)\pi/\omega\}$ leaves the Hamiltonian invariant and that $\Phi_\alpha(x,t+(2j+1)\pi/\omega)=\pm\Phi_\alpha(x,t)$; the states Φ_α must have either odd or even generalized parity (GP) [8].

Generalized parity leads to selection rules for the integrals appearing in Eq. (11). We find that

$$\int_{-\infty}^{\infty}dx\ C^*(n,x;\alpha)xC(m,x;\beta)=0 \tag{12}$$

[if $\mathcal{P}_G(\alpha)=\mathcal{P}_G(\beta)$ and $n-m$ is even, or if $\mathcal{P}_G(\alpha)\neq\mathcal{P}_G(\beta)$ and $n-m$ is odd]. Moreover,

$$\begin{aligned}&\int_{-\infty}^{-L/2}dx\ C^*(n,x;\alpha)C(m,x;\beta)\\&\qquad=\int_{L/2}^{\infty}dx\ C^*(n,x;\alpha)C(m,x;\beta)\end{aligned} \tag{13}$$

(if $\mathcal{P}_G(\alpha)=\mathcal{P}_G(\beta)$ and $n-m$ is even, or if $\mathcal{P}_G(\alpha)\neq\mathcal{P}_G(\beta)$ and $n-m$ is odd). Here $\mathcal{P}_G(\alpha)$ denotes the generalized parity of the Floquet state Φ_α whose Fourier coefficients $C(n,x;\alpha)$ appear in the integrals.

Equation (11) shows that the shifting frequencies $\Delta_{\alpha,\beta}$ introduced in Sec. VI are differences between the quasien-

ergies (i.e., $\Delta_{\alpha,\beta}=\varepsilon_\beta-\varepsilon_\alpha$). The points of accidental degeneracy (i.e., the $\{\omega,I\}$ points for which $\Delta_{\alpha,\beta}=0$) turn out to be the points where two quasienergies become equal. The connection between the equality of the quasienergies and localization was established in Ref. [2]. Here we focus mainly on EHG and LFG. We see that EHG appears and LFG disappears when two quasienergies become degenerate. Moreover, the symmetry rules (12) and (13) ought to explain whey we see no pure even harmonics when the parameters are not AD points, and no shifted odd harmonics regardless of the laser frequency and intensity.

We examine first the case when the Floquet states contributing to Eq. (11) are not accidentally degenerate. The static part of the observable $O(t)$ is obtained from Eq. (15) when $n=m$ and $\alpha=\beta$, and has the form

$$O_1=\sum_{\alpha=1}^{\infty}|A_\alpha|^2\int_{-\infty}^{\infty}dx\ C^*(n,x;\alpha)O(x)C(n,x;\alpha)\ . \quad (14)$$

If we replace O with μ in Eq. (14), we obtain the static part μ_1 of the dipole. Because of the symmetry rule Eq. (12), μ_1 is zero. Symmetry also allows us to make a statement about the static part of the probability that the electron is localized in a well. According to the symmetry rule Eq. (13), $P_{L,1}=P_{R,1}$; this means that the zero-frequency component of the electron density is equally distributed among the two wells. This is consistent with the fact that the zero-frequency component of the dipole is zero. This has an interesting consequence: in the absence of AD, the laser cannot localize the electron regardless of the pulse shape, laser phase, or the nature of the initial conditions. Indeed, localization in a well (the left one, for example) means that the probability $P_L(t)$ is substantially larger than 0.5, *at all times*. This means that the static part $P_{L,1}$ of $P_L(t)$ must be larger than 0.5. However, the equality $P_{L,1}=P_{R,1}$ and the fact that these probabilities must add up to 1, precludes this. The fact that the degeneracy of the quasienergies is related to localization has been shown previously [2].

The purely harmonic term

$$O_2(t)=\sum_{n=-\infty}^{\infty}\sum_{m=-\infty}^{\infty}(1-\delta_{nm})\exp[i(m-n)\omega t]\times\sum_{\alpha=1}^{\infty}|A_\alpha|^2\int_{-\infty}^{\infty}dx\ C^*(n,x;\alpha)\times O(x)C(m,x;\beta) \quad (15)$$

originates from Eq. (11) when $n\neq m$ and $\alpha=\beta$. If $O(x)$ is the dipole operator, the selection rule Eq. (12) indicates that the integral in Eq. (15) is zero for $n-m$ even. Thus, in the absence of AD, the induced dipole will have no even harmonics. There is no symmetry rule preventing odd harmonics. Obviously, even harmonics can be observed, if at all, only at points of accidental degeneracy.

The shifted-harmonic term

$$O_3(t)=\sum_{\alpha=1}^{\infty}\sum_{\beta=1}^{\infty}A_\alpha^*A_\beta^*\exp[-i(\varepsilon_\beta-\varepsilon_\alpha)t](1-\delta_{\alpha,\beta})\times\sum_{n=-\infty}^{\infty}\sum_{m=-\infty}^{\infty}(1-\delta_{n,m})\exp[i(m-n)\omega t]\times\int_{-\infty}^{\infty}dx\ C^*(n,x;\alpha)O(x)\times C(m,x;\beta) \quad (16)$$

corresponds to $n\neq m$ and $\alpha\neq\beta$ in Eq. (11). The integrals in Eq. (16) are zero if the states α and β have the same GP and $n-m$ is even. If α and β have different GP's, the integrals are zero if $n-m$ is odd. Thus, we expect each pair of Floquet states α and β to generate a progression of doublets of the form $n\omega\pm(\varepsilon_\alpha-\varepsilon_\beta)$; if α and β have the same parity, n is odd; if they have different parity, n is even.

The bandhead term

$$O_4(t)=\sum_{\alpha=1}^{\infty}\sum_{\beta=1}^{\infty}A_\alpha^*A_\beta\exp[-i(\varepsilon_\beta-\varepsilon_\alpha)t](1-\delta_{\alpha\beta})\times\sum_{n=-\infty}^{\infty}\int_{-\infty}^{\infty}dx\ C^*(n,x;\alpha)O(x)\times C(n,x;\beta) \quad (17)$$

originates from Eq. (15) when $n=m$ and $\alpha\neq\beta$. Since the quasienergies depend on $\{\omega,I\}$, the difference $(\varepsilon_\alpha-\varepsilon_\beta)$ can be made small; the bandhead term will oscillate at very low frequency, thus generating LFG. This happens, for example, when $\{\omega,I\}$ approaches a point of accidental degeneracy. If O is the dipole operator, the integrals in Eq. (17) are zero unless $C^*(n,x;\alpha)$ and $C(n,x;\beta)$ have different GP's.

It is difficult to compare in a precise way the height of the LFG peak to that of the other peaks in $\mu(\Omega)$ because these quantities depend on both the amplitudes A_α, $\alpha=1,2,\ldots$ and on the integrals over the Floquet states. However, the LFG intensity ought to be high if the electron wave function, written as in Eq. (10), is essentially a coherent superposition of two nearly degenerate Floquet states with different GP's and with nearly equal amplitudes A_α. An electron in such a state drifts slowly from one well to another, and at some times during its travels has a high probability of being in one of the wells.

We can now examine the case when two of the Floquet states describing the electron wave function are accidentally degenerate, that is, when

$$\Delta_{\alpha,\beta}=\varepsilon_\alpha(\omega,I)-\varepsilon_\beta(\omega,I)=0\ . \quad (18)$$

The condition

$$\varepsilon_\beta+n\omega=\varepsilon_\alpha+m\omega\ , \quad (19)$$

where n and m are integers, affects $\mu(t)$ in the same way as (18); moreover, it includes (18) as a limiting case. Therefore, defining accidental degeneracy by (19) is more general. However, in examining the numerical results reported here, we found condition (18) to be more useful;

for the parameters used by us, the condition (19) was never satisfied except when $n=m$, which leads to (18). For this reason, we prefer to use the definition (18) and examine its consequences in what follows. Arguments of a similar type will determine the properties of $\mu(\Omega)$ when (19) is satisfied.

We now study what happens to various terms in $\mu(t)$ when $\{\omega,I\}$ approaches a point of accidental degeneracy. We have already shown that, for the dipole moment, the term μ_1 is zero because of the symmetry rules. The time evolution of the pure-harmonic term does not depend on $\varepsilon_\beta-\varepsilon_\alpha$ and it is therefore unaffected as $\{\omega,I\}$ approaches an AD point. The integrals and the amplitudes A_α may change, but this is likely to be a smooth change with $\{\omega,I\}$. We have already shown that the pure-harmonic term has only odd harmonics, and thus we must conclude that AD is likely to cause only minor changes in the odd harmonics in $\mu(\Omega)$.

As $\Delta_{\alpha,\beta}\rightarrow 0$ for a pair of states α and β, the contribution of these states to the shifted-harmonic part $O_3(t)$ becomes pure harmonic. The selection rules are as follows; If the two states about to become accidentally degenerate have the same GP's, then the corresponding shifted-harmonic term evolves into a pure odd harmonic. If the states have different GP's they evolve into a pure even harmonic.

The bandhead term Eq. (17) also changes as $\{\omega,I\}$ approaches a point of accidental degeneracy for two states α and β: the oscillation frequency $(\varepsilon_\beta-\varepsilon_\alpha)\rightarrow 0$ goes to zero, and the bandhead term gives a static contribution to $O(t)$. The only nonzero contributions in the bandhead terms are those involving Floquet states with different GP's. Thus LFG is generated by a pair of nearly degenerate Floquet states of different generalized parity; the static dipole is generated when these states become degenerate.

We can also use this theory to examine the connection between localization and spectroscopic properties. As we pointed out, to have localization, $P_L(t)$ [or $P_R(t)$] must have a sizable static component $P_{L,1}$. Localization is also associated with a large static dipole. We have shown that $\mu(t)$ can have a static dipole only if a pair of Floquet states with different GP's—which appear in the electron wave-function expansion (13)—become accidentally degenerate. The static parts μ_1 or $P_{L,1}$ can be a large fraction of $\mu(t)$ or $P_L(t)$ only if the electron wave function is dominated by these two states. Strong localization means that the system can be described fairly well by two degenerate Floquet states with different GP's. The same conclusion was reached in Ref. [2].

To confirm this interpretation and provide further insights into the manner in which the the Floquet representation leads to a simple explanation of the numerical calculation, we have calculated the quasienergies of the Floquet states that contribute to the electron wave function of the four examples presented in Figs. 7 and 8. Using Eq. (14), we can show that the transform

$$C(\Omega)=2\,\mathrm{Re}\left[\int_{-\infty}^{\infty} dt\, e^{-i\Omega t}W(t-t')C(t)\right] \tag{20}$$

of the overlap integral

$$C(t)=\langle\Psi,t=0|\Psi,t\rangle = \sum_{n=-\infty}^{\infty}\sum_{\alpha=1}^{\infty}\exp[i(\varepsilon_\alpha+n\omega)t] \times\left[A_\alpha\int dx\, C(n,x;\alpha)\Psi(x,t=0)\right] \tag{21}$$

has peaks at the frequencies $\varepsilon_\alpha+n\omega$. Furthermore, if the peak corresponding to the frequency $\varepsilon_\alpha+n\omega$ is high, then the Floquet state $c(n,x;\alpha)$ contributes importantly in the representation of both the initial electron state and the time-dependent state created by driving the system with the laser. Equation (25) is valid only at those times when the laser amplitude has become constant. For this reason, we use in (20) a window function W chosen to confine the integration to that time domain. Since W is a Gaussian, the transform has Gaussian peaks centered at the energies $\varepsilon_\alpha+n\omega$. In all figures, we show the peak position and height.

Figure 9 and 10 show the transforms of the overlap integrals for a system driven under the conditions used in Figs. 7 and 8. We examine first the case of the less intense laser [Figs. 9(a) and 10(a)]. In Fig. 9(a), the system has two Floquet states with the quasienergies $\varepsilon_1=125.4$ cm^{-1} and $\varepsilon_2=161.4$ cm^{-1}. Their difference $\varepsilon_2-\varepsilon_1=36$ cm^{-1} is—as expected from our analysis—equal to the

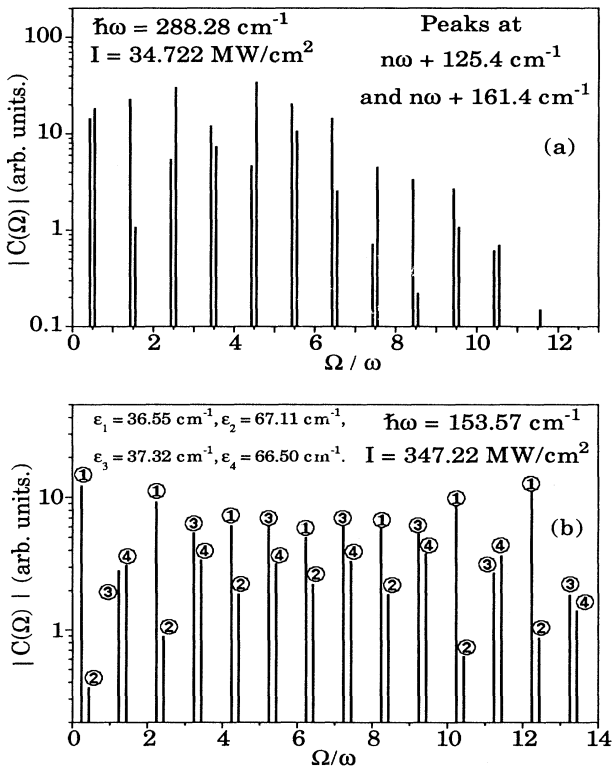

FIG. 9. Fourier transforms of the correlation function [see Eq. (24)] for the cases shown in Fig. 7. (a) contains two quasienergies and (b) contains four.

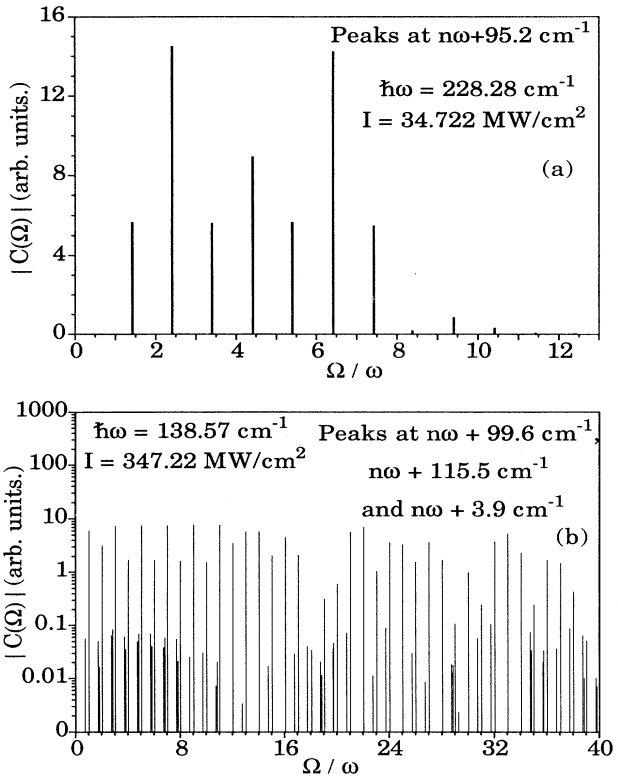

FIG. 10. Fourier transforms of the correlation function for the cases shown in Fig. 8. (b) contains mainly the two quasienergies $\varepsilon_1=99.6$ cm^{-1} and $\varepsilon_2=3.9$ cm^{-1}. Other peaks are much weaker (note the logarithmic scale).

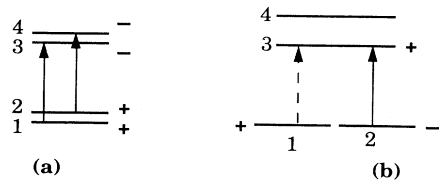

FIG. 11. Schematic diagram of the quasienergies.

frequency $\Delta_{1,2}$ appearing in the bandhead and in the shifted frequencies in $\mu(\Omega)$ [Fig. 7(a)].

Let us examine now Fig. 10(a). The plot shows that the electron wave function contains only one quasienergy. By changing the laser frequency from 288.28 cm^{-1} [Fig. 9(a)] to 228.28 cm^{-1} [Fig. 10(a)], we have shifted the quasienergies from $\varepsilon_1=161.4$ and $\varepsilon_2=125.4$ cm^{-1} [Fig. 9(a)] to $\varepsilon_1=95.2$ cm^{-1} and $\varepsilon_2=95.2$ cm^{-1} [Fig. 10(a)], and brought them into accidental degeneracy. In Fig. 8(a), which plots $\mu(\Omega)$ for the same conditions as in Fig. 10(a), we see that EHG is present, there is no LFG, and there is large static dipole (not shown in the figure), as predicted by our analysis.

The situation in Fig. 9(b), which corresponds to a higher laser intensity, is more complicated. The wave function has four Floquet components having the energies $\varepsilon_1=36.55$ cm^{-1}, $\varepsilon_2=37.32$ cm^{-1}, $\varepsilon_3=66.50$ cm^{-1}, and $\varepsilon_4=67.11$ cm^{-1}. These could, in principle, pair up to give a large number of lines in $\mu(\Omega)$. However, $\mu(\Omega)$ [in Fig. 7(b)] has fewer lines than expected: one bandhead, one progression of even shifted harmonics, and a progression of odd pure harmonics. This discrepancy can be explained as follows. Let us assume that the four states have the parity indicated in Fig. 11(a). For what follows, it is only important that the states in one doublet have the same parity and the states in different doublets have different parities. The selection rules allow only a pair of states with different parities to generate bandheads and shifted even harmonics. This means that the only bandhead frequencies are $\Delta_{3,1}=\varepsilon_3-\varepsilon_1=(66.50-36.55)\,\text{cm}^{-1}=29.95$ cm^{-1}, and $\Delta_{4,2}=\varepsilon_4-\varepsilon_2=(67.11-37.32)\,\text{cm}^{-1}=29.79$ cm^{-1}. The frequencies of these two bandheads and of the accompanying shifted even-harmonic progressions are too close to be resolved in our calculation. To see them in the Fourier transform of $\mu(\Omega)$, we would have to use a very broad window function (in the time domain) and to calculate $\mu(t)$ for a very long time.

According to the selection rules, only a pair of Floquet states with the same parity will generate shifted odd harmonics. In the case shown in Fig. 11(a), this gives the shift frequencies $\Delta_{2,1}=37.22-36.55=0.67$ cm^{-1} and $\Delta_{4,3}=67.11-66.50=0.61$ cm^{-1}, which are too small to be resolved when $\mu(\Omega)$ is calculated.

We examine now Fig. 10(b), which corresponds to the same intensity as Fig. 9(b), but a slightly different frequency. This slight change in frequency causes the change in number of quasienergies needed to describe the dynamics of the electron from four to three. These are $\varepsilon_1=3.9$ cm^{-1}, $\varepsilon_2=99.6$ cm^{-1}, and $\varepsilon_3=115.5$ cm^{-1}. The change in the number of quasienergies suggests that two states are accidentally degenerate. This is confirmed by the presence of even harmonics in Fig. 8(b), which shows $\mu(\Omega)$ calculated for the same conditions as in Fig. 10(b). The major features in Fig. 8(b) are one bandhead at 95.5 cm^{-1}, a shifted even-harmonic progression, and a shifted odd-harmonic progression, both having the shifting frequency 95.5 cm^{-1}. There are a few other lines in the spectrum, but they do not form intense progressions with many lines in them. The dominant features of the spectrum can be understood from Fig. 11(b). To give even harmonics, the degenerate states must have different parity. If the parity of the state 3 is +, it can pair up with the degenerate state 1, having the same parity, and give a shifted odd-harmonic progression with the frequencies $(2n+1)\omega\pm(99.6-3.9)$ cm^{-1}; the pair 3 and 2 gives shifted even harmonics with the frequencies $(2n+1)\omega\pm(99.6-3.9)\,\text{cm}^{-1}$. These explain the main features in $\mu(\Omega)$. The other pairs of states will generate other lines in $\mu(\Omega)$, and they do. However, there are not enough lines to assign them to specific progressions.

The analysis presented here agrees with and explains the rules derived empirically in Sec. IV; it also provides an explanation for the "data" generated by solving numerically the time-dependent Schrödinger equations.

The conclusions of this analysis are summarized in Sec. VIII.

VIII. SUMMARY AND DISCUSSION

The numerical results obtained here are best summarized by using as a framework the analysis presented in Sec. VII. One can describe the time evolution of the dipole $\mu(t)$, in the time interval when the laser amplitude is constant, by expanding the electron wave function in terms of the Floquet states of the system. After this is done, $\mu(t)$ is a sum of terms having a time dependence of the form $\exp\{i\Omega[\alpha,\beta,(n-m)]t\}$. Here α and β label the Floquet states $\Phi_\alpha(x,t)$ and $\Phi_\beta(x,t)$ appearing in Eq. (9), and n (and m) label the corresponding Floquet modes [see Eq. (10)]. The frequencies in the exponentials have the general form

$$\Omega(\alpha,\beta,n-m)=\varepsilon_\alpha(\omega,I)-\varepsilon_\beta(\omega,I)+(n-m)\omega \ . \quad (22)$$

The real functions $\varepsilon_\alpha(\omega,I)$ are the quasienergies of the Floquet states $\Phi_\alpha(x,t)$, and n and m are integers.

For most laser frequencies and intensities, the quasienergies are not degenerate, and we use this to classify the terms appearing in $\mu(t)$. The case when a pair of states is degenerate is very interesting and will be examined as a limiting case. When all quasienergies of the Floquet states needed to describe the electron wave functions differ from each other, we can write the dipole as the sum of four terms, each term having a different type of time dependence.

The static term corresponds to $\alpha=\beta$ and $n=m$, and is independent of time. For the symmetric Hamiltonian used here (i.e., invariant to $x\rightarrow -x$), this term is zero. Thus, for most values of the parameters $\{\omega,I\}$, for which quasienergies are not degenerate, the system has no static dipole. This also means that the electron is not localized.

The pure-harmonic term corresponds to $\alpha=\beta$ and $n\neq m$, and it has Fourier components at the frequencies $\Omega(\alpha,\alpha,n-m)=(n-m)\omega$. For a symmetric well, there are no terms with even frequencies, hence no even harmonics in the spectrum.

The shifted-harmonic term corresponds to $\alpha\neq\beta$ and $n\neq m$, and every pair of Floquet states α and β generates a progression of doublets at $(n-m)\omega\pm[\varepsilon_\alpha(\omega,I)-\varepsilon_\beta(\omega,I)]$. If α and β have different generalized parity, the terms with $n-m$ odd are forbidden by symmetry; if α and β have the same GP, then the terms with $n-m$ even are forbidden.

Finally, the fourth type of term corresponds to $\alpha\neq\beta$ and $n=m$. They oscillate with the frequency $\Omega(\alpha,\beta,n-m=0)=\varepsilon_\alpha(\omega,I)-\varepsilon_\beta(\omega,I)$, and we call them the bandhead terms. Only pairs of states α and β having different generalized parity can generate bandhead terms.

In our calculations, we have observed that at moderate laser powers (e.g., 34.722 MW/cm^2), the wave function can be described by two Floquet states of different parity. In this case, the above rules predict that the spectrum of $\mu(t)$ consists of a bandhead, a progression of shifted even harmonics, a progression of pure odd harmonics, no static dipole, and no permanent (i.e., time-independent) localization of the electron. These predictions are confirmed in all our calculations.

As the parameters $\{\omega,I\}$ are changed to approach a point at which the quasienergies of two Floquet states α and β having different GP's become degenerate the spectrum of $\mu(t)$ changes. The frequency of the bandhead term becomes smaller and smaller and goes to zero. This is responsible for the low-frequency generation observed in the spectrum. When the accidental degeneracy takes place, the LFG frequency becomes zero and generates a static dipole. If the electron wave function is dominated by the two states becoming degenerate and if the amplitudes of these two states are comparable, the accidental degeneracy leads to localization. Furthermore, the shifted-harmonic term consisting of a progress of doublets having the frequencies $2n\omega\pm[\varepsilon_\alpha(\omega,I)-\varepsilon_\beta(\omega,I)]$ collapse, as $\{\omega,I\}$ approaches the point of accidental degeneracy of two states with different GP's to a progression of even harmonics of frequency $2n$.

If the Floquet states becoming degenerate have the same parity (this has not happened in our calculations and there may be a noncrossing rule preventing such degeneracy), the behavior of $\mu(t)$ is different. The bandhead frequency is not affected, and the progression of odd shifted harmonics becomes a pure odd harmonic. No static dipole, even-harmonic generation, or localization will be observed.

We will now discuss the possibility of observing these effects experimentally. The fact that our model is only a schematic representation of a double quantum well causes some uncertainty. The low-frequency and the even-harmonic generation are most intense when the electron wave function is a linear combination of two floquet states and the laser shifts their quasienergies into degeneracy. All factors diminishing the coherence of these two states will diminish the magnitude of EHG and LFG below that predicted by our model. The effect of the static imperfections in the structure are the easiest to understand. The state of electron is a wave packet localized within the coherence length of the electron. Different electrons in the dilute electron gas in the wells are localized in different spatial regions, each having a slightly different Hamiltonian and slightly different Floquet states. Therefore it is not possible to find values of $\{\omega,I\}$ that will be simultaneously the Floquet states of all these electrons into accidental degeneracy. Some will be degenerate, some nearly degenerate. The degenerate ones will produce a static dipole, progression of pure odd and harmonics, and one of pure even harmonics; the nearly degenerate ones will produce a very-low-frequency component, pure odd harmonics, and doublets with a small splitting around the even-harmonic frequencies. If the measurements have low-frequency resolution these lines will be lumped together, and their intensity will be as high as if the structure is perfectly homogeneous. Poor homogeneity does not affect radically the low-resolution Fourier transform of the dipole.

Another source of dephasing comes from the existence of phonons. The initial state will consist of the product of an electron state and a phonon state, and the latter will be occupied thermally. This uncertainty in the initial energy will have the same effect as the inhomogeneous

broadening. Phonon-mediated transitions from one electron state to another (through the electron-phonon coupling) provide another dephasing mechanism. This will destroy coherent processes, such as localization, EHG, and LFG, on a time scale set by the inverse of the transition rate. This dephasing will broaden the LFG and EHG peaks in the Fourier transform of μ. This, of course, will diminish the intensity of high-resolution measurements. Both phonon-induced effects can be diminished by lowering the temperature and by performing low-resolution (in the frequency domain) measurements.

Even if perfect structures at 0 K can be used, the effects described here are not easy to detect experimentally. Making the semi-infinite Gaussian pulses with low frequency and a fast rise time required here is difficult. For example, if the electron is driven by a semi-infinite Gaussian pulse, the frequency must be smaller than the energy difference between the lowest states of the electron in the absence of the laser, and the rise time of the pulse of the order of 20 optical cycles.

The theory explaining these phenomena is fairly general, and therefore these effects need not be confined to quantum wells or to double wells. Other systems—such as atoms and molecules—in which inhomogeneity and dephasing are much easier to control, might show even-harmonic and low-frequency generation at laser frequencies for which better pulse-shaping technology is available.

ACKNOWLEDGMENTS

We are grateful to Jim Allen, Walter Kohn, Martin Hothaus, and Yuri Dakhnovskii for useful discussions. This work was supported by NSF Grant No. CHE-9112926.

*Address for correspondence.

[1] G. Bastard, *Wave Mechanics Applied to Semiconductor Heterostructures* (Halsted, New York, 1988); C. W. J. Beenakker and R. Van Houten, in *Semiconductor Heterostructures and Nanostructures,* edited by G. Ehrenreich and D. Turnbull (Academic, New York, 1991).

[2] (a) F. Grossmann, T. Dittrich, and P. Hanggi, Phys. Rev. Lett. **67**, 516 (1991) ; (b) F. Grossmann, T. Dittrich, and P. Hanggi, Physica B **175**, 293 (1991); (c) F. Grossmann, P. Jung, T. Dittrich, and P. Hänggi, Z. Phys. B **85**, 315 (1991); (d) F. Grossmann and P. Hänggi, Europhys. Lett. **18**, 571 (1992).

[3] Throughout this article, and the adjective bare indicates the properties of the system in the absence of the laser.

[4] D. Neuhauser (unpublished); M. Holthaus, Phys. Rev. Lett. **69**, 1596 (1992); R. Bavlli and H. Metiu, Phys. Rev. Lett. **69**, 1986 (1992).

[5] (a) J. A. Fleck Jr., J. R. Morris, and M. D. Feit, Appl. Phys. **10**, 129 (1976); (b) M. D. Feit, J. A. Fleck, Jr., and A. Steiger, J. Comput. Phys. **47**, 412 (1982); (c) M. D. Feit and J. A. Fleck, Jr., J. Chem. Phys. **78**, 2578 (1984).

[6] R. Heather and H. Metiu, J. Chem. Phys. **86**, 5009 (1987).

[7] J. H. Shirley, Phys. Rev. **138**, B979 (1965); S.-I. Chu, Adv. At. Mol. Phys. **21**, 197 (1985).

[8] We use the term generalized parity to distinguish from the transformation $x \rightarrow -x$.